NATURAL RADIATION CONTRIBUTION TO RENEWABLE ENERGY SEARCHINGE

Miguel Balcazar[1], Arturo Lopez, Magaly Flores[2] and Marciano Huerta

[1] Instituto Nacional de Investigaciones Nucleares, Apartado Postal 18-102, México DF 11801, México. miguel.balcazar@inin.gob.mx

[2] Gerencia de Proyectos Geotermoeléctricos, Comisión Federal de Electricidad, Alejandro Volta 655, CP 58290, Morelia, Michoacán, México.

Abstract

High anomalies of naturally occurring radon in geothermal fields are becoming an additional geophysics tool for determining the areas of geothermal activity underground. Under close collaboration with the Federal Electricity Board in Mexico (CFE), we have study four geothermal fields (Los Azufres, Tres Vírgenes, Humeros and Acoculco) for extending the energy potentially. The heat source in hydrothermal systems produces geothermal gasses, which transport radon to the surface faster than the common diffusion process in absence of a geothermal activity. This paper presents: mechanism of radon production, main physical and chemical features that make it an excellent indicator for locating heat sources of geothermal reservoirs, the detection basis of in situ radon concentration using a high sensitive radiation chamber and the planning experimental strategy for successful use of this technique.

Keywords: Radon; Geothermal energy; natural radiation; permeability.

1.- INTRODUCTION

The energy demand is closely related to population growth; however the energy production processes must fulfill with characteristics of sustainability, and the reduction of the emission of greenhouse gases caused by the use of fossil fuels. Alternative energy sources include geothermal energy; four countries, United States of America, Philippines, Indonesia and Mexico, have an installed capacity of 6,600 MW, which accounts for 70% of the total global installed capacity of geothermal energy [Akerblom 1997].

The geothermal energy potential lies in those geological places of high tectonic and consequently volcanic activity. Both conditions locate fragments of eruptive magma in regions close to the earth surface. If also in these regions occur hydrothermal processes that favor the presence of deep reservoirs, confined and recharged by meteoric water processes, it is possible that confined water (2 km to 3 Km deep) reaches temperatures above 200 °C due to heat transport by convection from the eruptive magma source.

To exploit this renewable energy resource, it is necessary to locate these reservoirs, drilling wells down to 2 km and 3 km deep to extract the steam generator of energy. Drillings are costly and prior to them is necessary to define the region most likely to be drill. The usual sequence for geothermal prospecting is the following: first a regional geological study determines the presence of volcanic structures and associated systems of faults defining the probable regional area. Then, geophysical surveys are conducted in the defined area; among them are gravimetric method which determines the density of the geological material at depth, establishing the presence of rocks and basins; magnetism that confirms the presence of magnetic material and possible warming of the rocks when; electrical resistivity whose minimum values locate areas at different depths with high presence of saline chemical compounds due to geochemical gas emissions; local seismicity allowing fault location. Next geochemical studies of springs (if any) identify substance called geo-thermometers, which forms only if the temperature of the reservoir is above well-defined high thresholds.

The reduction of oil sources and the greenhouse effect requires the use of alternative energy sources in Mexico. Amongst the widely alternative energy is geothermal energy

that has been in operation since 30 years ago. Location of the four main geothermal fields in Mexico is at Cerro Prieto, Baja California Norte; Tres Vírgenes, Baja California Sur; Los Azufres, Michoacán and Los Humeros, Puebla. All geothermal fields in Mexico correspond to hydrothermal type with a total installed capacity of 958 MW [Santoyo 2010] and are situated in the so called neo volcanic belt, which is an active volcanic formation situated from the northwest to the south east part of the country; however, it is partially characterized, requiring additional studies to identify its potential. Large geothermal potential sites are located in this neo volcanic belt where plans are underway to increase energy production. The Government of Mexico Put Forward a 15 years program named National Strategy of Energy 2013-2027 (ENE) to reduce the environmental impact of the energy sector through the so-called clean energy, giving priority to the increase in non-fossil technologies.

According to Maya-Gonzalez [2007] the prospecting strategy of geothermal fields includes six steps: regional survey; geology and geochemistry; geophysics; exploration wells; producing wells and building power station. Each step increases roughly its cost and its success ten times of the previous step [Maya-Gonzalez 2007]. Therefore, the success in each step depends of the quality of the data and its interpretation.

Geophysics survey includes: micro seismicity to evaluate activity of faults and fractures; electric conductivity which reveals the presence of the reservoir by detection at different depths the distribution of saline substances transported by geo gases up to the field surface; local gravitation anomalies to distinguish density of materials beneath the surface. Amongst these geophysical methods are radon anomalies at the surface of the field, which reveals permeable areas that are correlated to the other geophysical parameters to better characterization of the field under prospecting.

Radon migration models reasonable explain radon entry in houses [Jönsson 1997], mainly as a diffusivity transport through porous media; they also explain the enhanced migration by adding a pressure difference under controlled laboratory experiments [Van de Graff 1997] that create an advection transport. However, when dealing with radon migration to

the surface of an active geothermal reservoir, the thermodynamically characteristics and the complex lithology feature generate a more complicated situation.

A conceptual explanation of the advantages of using radon for locating permeable areas in geothermal fields under prospecting is given in this paper supported by experimental results. Along the paper some key questions are answered, amongst them are: How close to do the measurements?; is there reproducibility of radon distribution in a geothermal field?; does radon distribution shows differences in geothermal activity?; what is the relationship of radon with other exploration methods (seismology, conductivity, geology)?; what are the advantages of radon in geothermal exploration?.

2.- RADON IN GEOTHERMAL FIELDS

Our group has developed a geophysical method as a complementary final stage of geothermal prospecting in areas defined by geology, geophysics and geochemistry. The method consists of determining the concentration of a natural radioisotope Radon-222 (^{222}Rn) which is transported to the surface by the geo-gases from the large thermodynamic activity from the hot reservoir.

Due to the short half-life of this natural tracer (3.8 days) its high concentration indicates sites of faults recently open and existing permeation of the field, which improves the understanding of resistivity, because saline substances in some areas could have been transported by geo-fluids through a previous permeation in the geothermal field which does not exist anymore. All these geological, geophysical and geochemical studies on the geothermal areas of interest are fed in a Geographical Information System (GIS) for interpretation and correlation with radon mapping.

2.1.- Radon migration

^{222}Rn is a decay product of Radium-226 (^{226}Ra); both belong to the natural radioactive chain of Uranium-238 (^{238}U). Uranium is naturally present in most minerals in

concentrations of a few ppm; 1 ppp of uranium results in 12.3 kBq kg^{-1} of radium [Akerblom 1997]; uranium is present in soil particles as very tiny grain minerals and together with radium, can be mechanical transported by water leaching minerals.

In a micro scale consideration, Figure 1 (left) summarize the radon generation process from a mineral grain containing a radium isotope whose excess energy of 4.867 MeV make it to decay emitting a radon atom and an alpha particle in opposite directions, taking 1.8% and 98.2% of the excess energy respectively. This means that only the radium decaying near the surface of the mineral grain or near the surface of water drop produces a radon entering into the pore space due to the short radon-ion and alpha particle ranges, 0.07 μm and 0.1 μm respectively; additionally to the emission process described, radon diffuse from mineral grains and water from inner depths enhancing radon concentration in air pore.

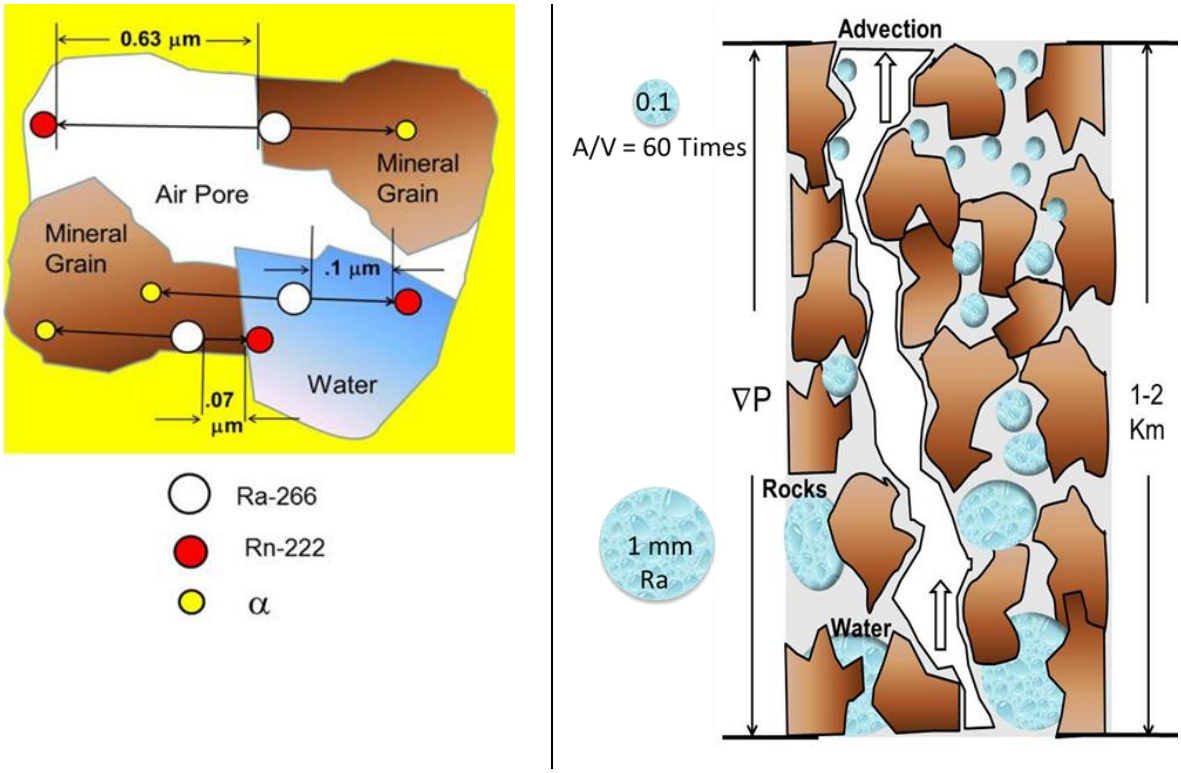

Figure 1.- Left: Radon in air pore comes from recoiled atom of radium decay in water and mineral grains. Right: Radon is transported by advection from deep the geothermal reservoir to earth surface easily through faults and sites of high permeable properties.

The radon concentration in a given pore space depends on the so-called soil emanation properties (radium concentration, grain size and porosity) and water emanation characteristics (radium concentration and water-drop radius); therefore, radon concentration in air pores increases with the exposed surface of cracks in rocks and with the reduce size of water drops.

Despite of miniature diffusion process, radon is an excellent natural radioactive tracer of hydrothermal reservoirs in geothermal energy prospecting, because radon transport phenomena, rather than the diffusion one, is a dominant radon migration process, due to the high pressure and temperature gradients in the geothermal field, resulting in high radon concentrations at the surface of geothermal field. In a macro scale approach, Figure 1 (right) shows that once radon is in the air pore, it is transported together with other geo gasses as CO_2, H_2, N_2 and CH_4 by advection mechanism in the upward direction, due to the enormous pressure gradient produced by the thermodynamically activity of the geothermal reservoir as deep as 1 km to 3 km.

As geothermal fluids are transported to the surface, there is an additional radon contribution into the air pore from the radium decay in water because reduction in water pressure atomize water drops reducing its radius r and increasing the ratio area A to volume V in the water drops, this is $A/V = 3/r$; therefore a water radius reduction of one order of magnitude means 60 times increase A/V ratio increasing radon emanation from radium decay in water as it is shown in Figure 1 (right). Because radium can be leached from the mineral source its origin depends on the water mobility underground, having a greater transport in an active geothermal reservoir.

These two last characteristics, cracks and small water drops, are significantly enhanced in a geothermal field, having a deep hydrothermal reservoir, whose presence along several thousands of years, have produced cracks (faults and fractures) in that area. The net corresponding effect is the increase of radon concentration on the top of those areas where a hydrothermal reservoir is present and the low radon concentration where there is not.

2.2.- Radon permeation indicator

Modeling the expected high radon concentration at the surface of the thermodynamically active geothermal reservoir is very complex, because in addition to radon generation and losses processes mentioned above, radon emanation depends on the diverse mineral types located in the lithology structure and the variable areas of the highly fractured geological structures. In spite of that, if there is geothermal activity underground in field under prospecting, there is significant radon transport by advection due to the big pressure and temperature gradients and gas carriers, being therefore transport the main migration process. The resulting is to have an area in the geothermal field with good permeability characteristics.

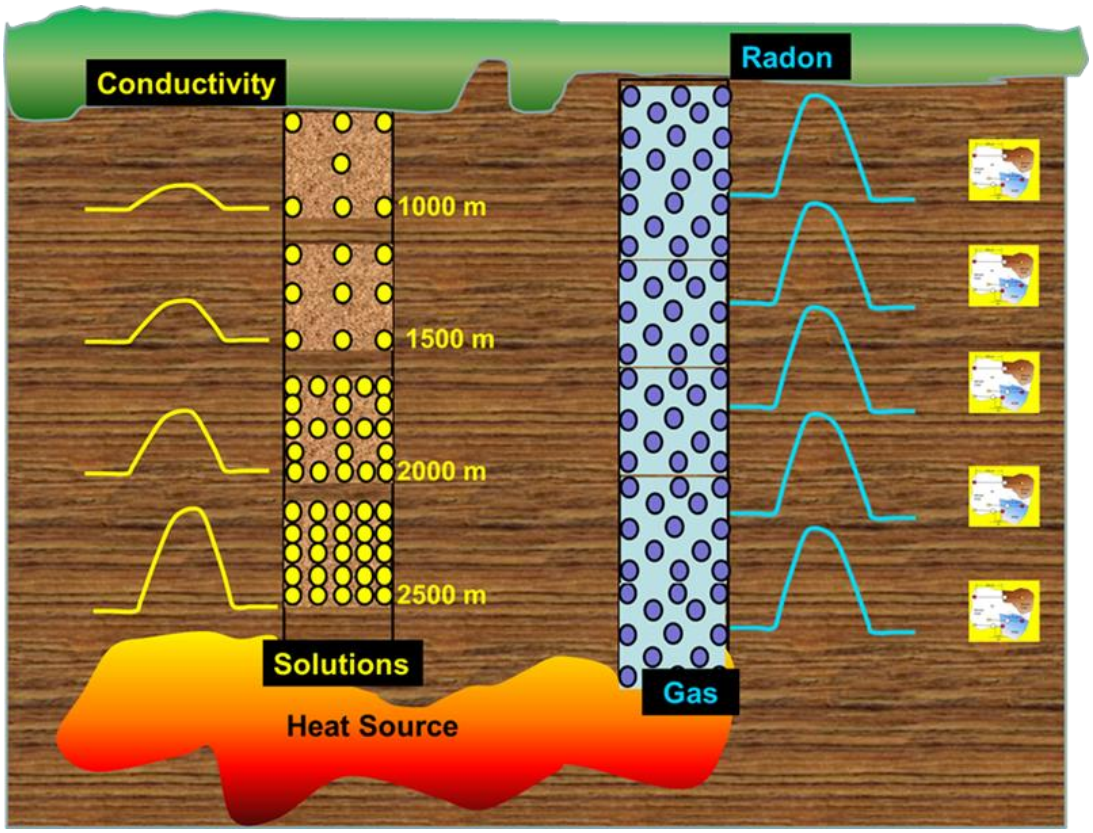

Figure 2.- Presence of alkaline solutions from the reservoir gradually reduce its concentration as they approach to the surface (left). Although radon from the reservoir decays as it is ascending to the surface, more radon is generated all along the way.

Part of radon originated from deep near the reservoir is lost in its traveling to the earth surface because radioactive decay, however this lost is compensated with radon originated all along the vertical column from the reservoir up to the earth surface during the advection process as it is appreciated in Figure 2 (right). This building effect on radon does not occur in the resistivity exploration technique, because the presence of alkaline solutions from the reservoir gradually reduce their concentration as they approach to the surface Figure 2 (left).

Figure 3 is simplified diagram to understand the relationship between the measurements of microsismicity (fractures), conductivity (inverse of resistivity) and radon in three hypothetical areas of a geothermal field: one with no fractures nor faults (A) and two with them (B, C).

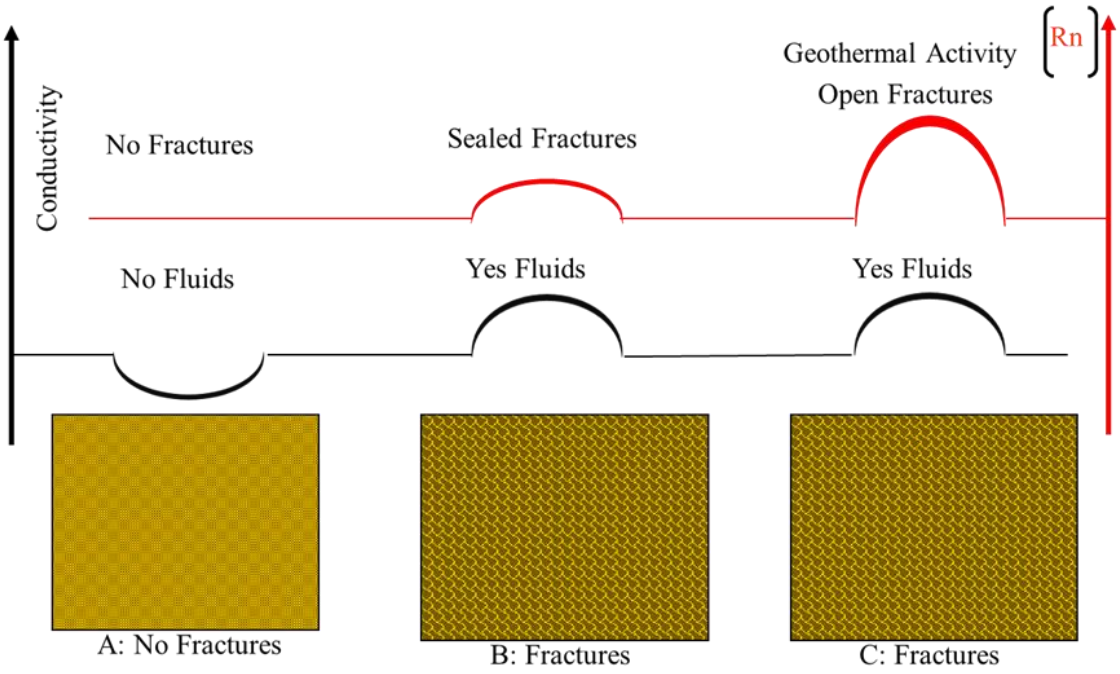

Figure 3.- Permeability properties as deduced from the relationship between conductivity, fractures and faults in the field and radon concentration.

Scare presence of geothermal fluids gives a low conductivity values (black line) in the low permeable area A with a low transport of radon to the surface (red line). In case B, fractures

although exist as determined by geology and microcosmic studies, at present they are sealed or partially sealed, however there is a good conductivity signal that comes from the alkaline material deposited before the factures were sealed; the corresponding low permeability is observed by the low radon concentration. In case C the open fractures and faults and the high permeability produce a high conductivity signal and high radon concentration.

The underground thermodynamic activity of the hot reservoir in geothermal fields is the sources of energy production and creates a pressure gradient higher than in absence of this hydrothermal activity.

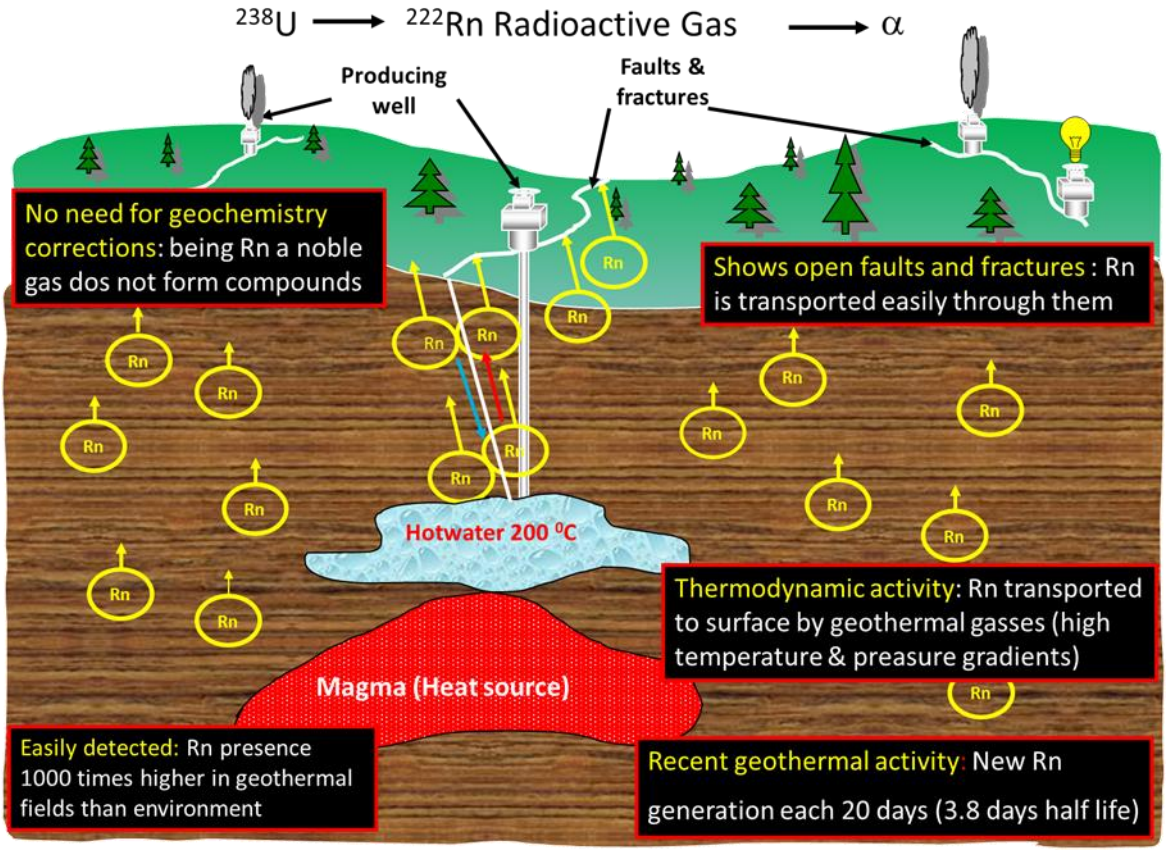

Figure 4.- Main radon properties for geothermal exploration.

The diagram in Figure 4 helps to summarize radon properties for its successfully use in geothermal exploration: The hydrothermal activity generates geo gasses that transport

radon to the earth surface faster than the diffusion process; radon is transported to the surface easily through open faults and fractures; because radon has a short half-life, radon shows the geothermal activity of the last 20 days; being radon a noble gas it does not form compounds and there is no need to for geochemistry corrections; radon is easy and fast to detect electronically in situ, it is present in concentrations up to 1000 times higher in geothermal fields than in environment.

2.3.- Radon evaluation

There are several challenges to overcome in determining the radon concentration in a geothermal field: the detector should be able to discriminate ^{222}Rn from ^{220}Rn; the detector should cover a wide range of radon concentration sensitivity; radon measurement procedure should permit to map hundreds of points in the geothermal field; radon detection in soil should avoid the undesired pressure difference in the soil-air which affects radon diffusion at the top surface of the field; and the grid mapping has to be optimized in size not to lose information nor to oversampling the field.

Radon has three isotopes, ^{219}Rn, ^{222}Rn, and ^{220}Rn; ^{219}Rn does not produce any interferences in the detection system for two reasons: firstly it comes from ^{235}U whose abundance in soil and rocks is 1/137 of that of ^{238}U (generator of ^{222}Rn); and secondly the half-life of ^{219}Rn is only 4 seconds which means that in about 24 seconds (six half-lifes) its concentration is reduced to about 3%. As far as ^{220}Rn is concerned, it comes from the decay series of Thorium-232 (^{232}Th), whose abundance can overcome of that of ^{238}U in ratios ^{232}Th/^{238}U as big as 8.2 for quartz monzonite and granite; the corresponding ^{220}Rn half-life is 56 seconds, therefore any detection system has to suppress ^{220}Rn contribution from that of ^{222}Rn. Two kinds of detectors were used for determining radon concentration in the field: plastic detectors capable of permanently recording the damage of alpha particles from radon and a high sensitivity ionization chamber.

3.- MATERIALS AND METHODS

3.1.- Plastic detectors

LR-115 plastic detector (made by Kodak Pathé, France) is composed by a red-sensitive-film 13 μm thick in contact with a non-sensitive-plastic 100 μm thick. The LR-115 detector is placed at the upper part of a PVC tube 30 cm long, which it is located inside another PVC tube buried at 1 m below the earth surface to overcome the undesired pressure difference at the surface, see diagram and pictures in Figure 5 (left). The 30 cm distance from the soil to the detector allows ^{220}Rn to decay before reaching the plastic detector. The LR-115 plastic detector register the alpha particle damage from radon as holes (see Figure 5 upper right), once the plastic has been subject to chemical corrosion [Balcazar 1991], which reduces the initial 13 μm thickness of the detector down to the so called residual thickness h. The experimental number of holes per cm^2 day ρ is proportional to the radon concentration [Rn]. Then, the ^{222}Rn concentration is given [Balcazar 1993] by the following expression:

$$[Rn] = \eta \left[\frac{37 \frac{Bq}{m^3}}{\frac{holes}{cm^2\ day}} \right] \frac{f(h)\rho\left[\frac{holes}{cm^2}\right]}{T\ days} \qquad (1)$$

Where: η is the detector efficiency determined at h = 4.5 microns, $f(h)$ is the correction factor for the residual thickness h of the plastic detector and has the following expression $f(h) = 0.041h^2 - 0.752h + 3.442$ [Balcazar 1993].

The experimental density of holes ρ is evaluated using a spark counter (see Figure 5 bottom right) [Balcazar 1984]; the maximum density of counting is 3000 holes/cm^2 to avoid hole overlapping; typical background of an unexposed plastic detector is 4 holes/cm^2. From equation 1 the upper limits of radon concentration [Rn] as function of residual thickness are

calculated and shown in Figure 6; the three upper curves correspond to an expected hole density of 3000 holes/cm^{-2} and an exposures time of one week (red squares), two weeks (green triangles) and one-month (violet dots). The lower detection value is considered as 40 holes/cm^2 for a period of one-month time.

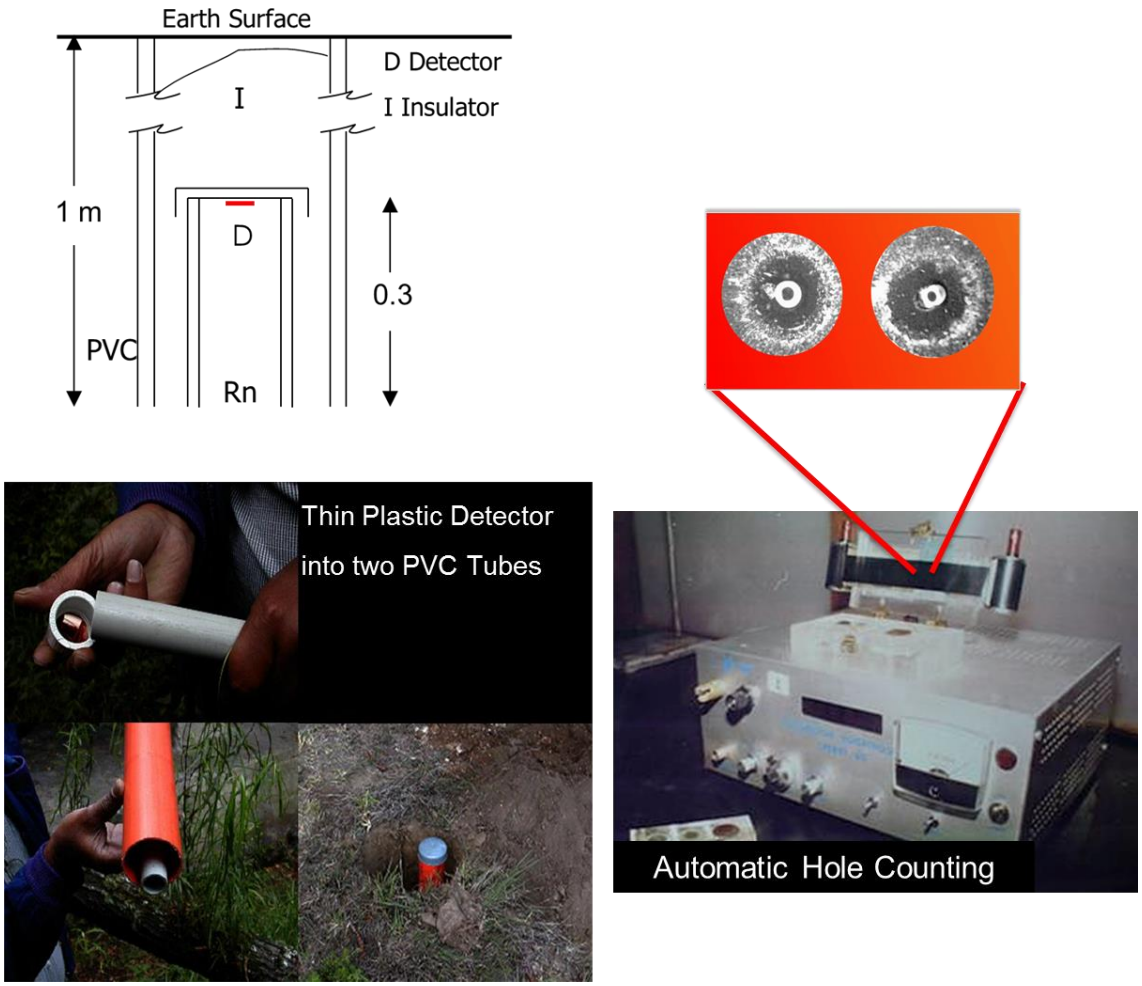

Figure 5.- Left: Diagram and pictures of plastic detector ensemble. Right: Holes in plastic detector produced by alpha interaction and automatic holes counter.

Table 1 shows three cases for residual thickness of 4.5 μm, 5.5 μm and 8 μm; each one display two extreme possibilities 40 and 3000 holes/cm^2, corresponding to counting errors of 16% and 2 % respectively.

Based on Table 1 the exposure time of plastic detectors in the geothermal field was no greater than 14 days, avoiding the difficulty of handling 4.5 μm residual thicknesses.

Table 1.- Upper and lower detection limits for plastic detectors

Detection limits LR115 [Rn] kBq m^{-3}						
	Residual Thickness of plastic detector h					
	4.5 μm		5.5 μm		8 μm	
Exposure time T	E 16 %	E 2%	E 16 %	E 2%	E 16 %	E 2%
7 days	0.23	17.67	0.37	28.49	3.19	240.50
14 days	0.12	10.30	0.19	16.59	1.68	140.15
30 days	0.05	4.12	0.08	6.64	0.72	56.06
Lower limit correspond to 40 holes/cm^2 with an expected error E of 16%. Upper limit correspond to 3000 holes/cm^2 with an expected error E of 2%.						

The wide range of experimental [Rn] displayed in Figure 6 ensures to cover all possible radon concentration in geothermal field without the worry of losing data. This detector ensemble is of particular importance when repetitive measurements have to be performed in the same area of a geothermal field because the 1 meter long PVC tube remains burrier in the ground and the change of new detector is easily and quickly introduced inside the 30 cm PVC tube. It is also cheap and fast to ensemble with local materials counting of detectors can be made with microscopes, image analyzers of even slide projectors.

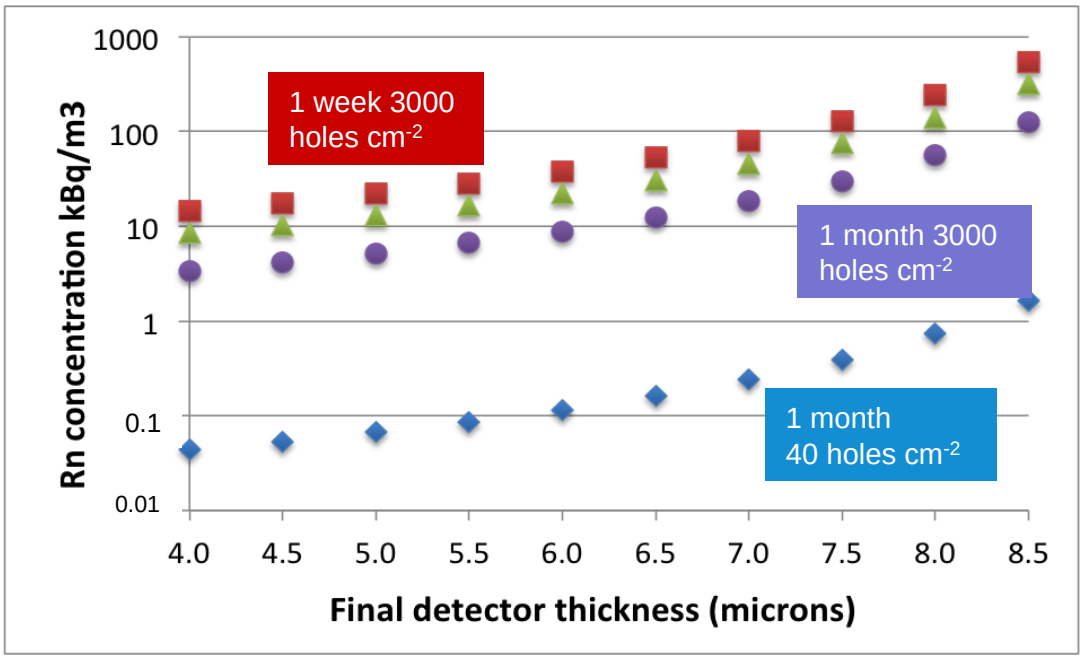

Figure 6.- Upper and lower detection limits for plastic detectors as function of the residual thickness.

3.2 Electronic detectors

An electronic detector ensemble AlphaGUARD (German made) permitted to determine radon concentration directly in the geothermal field. The ensemble is composed by a metallic soil-gas-prove, which is inserted 1 m below the earth surface, a battery operated pump, coupled the upper end of the soil-gas-prove by means of a plastic tube, extracts the air from the ground and injects it to a 0.56 l ionization chamber [Schubert *et al.*, 2015]. It has a wide linear measuring interval for ^{222}Rn from 2 Bq/m^3 up to 2000 kBq/m^3. Temperature and relative humidity operation limits are (-10 to +50) °C and (0 to 99) % respectively. The ionization chamber can selectively integrate the radon concentration in periods of (1 to 10) minutes or 60 minutes up to a maximum of 48,000 integration points, which are recorded in an internal memory together with temperature and humidity parameters, until they are down loaded in a computer for the corresponding analysis.

Because determination focuses on the ^{222}Rn concentration of the soil gas, collected data has to ensure that all ^{220}Rn from ^{232}Th has decayed before the actual radon concentration is

considered. Since ^{220}Rn has a half-life of 54 seconds, the decay of ^{220}Rn in a soil gas sample takes about 6 minutes (i.e. six half-lifes). After that period of time the radon concentration of the gas sample represents ^{222}Rn only. A typical spectrum of radon concentration determination is shown in Figure 7. The "Peak", which appears at the beginning of each plot, is formed by both ^{220}Rn + ^{222}Rn. After 6 minutes the ^{220}Rn disappears and a stable "concentration plateau" develops. That "concentration plateau" represents only the ^{222}Rn concentration of the soil gas.

Figure 7 (left) shows that ^{220}Rn + ^{222}Rn reach a concentration of about 30 kBq/m^3, at minute two, where the beginning of ^{220}Rn decay is followed by a constant ^{222}Rn concentration from minute six resulting in a ^{222}Rn concentration of about 13 Bq/m^3. Radon spectra at Figure 7 (right) shows a more dramatic example where the abundance of ^{220}Rn from ^{232}Th is so high that both ^{220}Rn + ^{222}Rn reach a concentration of nearly 50 kBq/m^3; however after six minutes the measured ^{222}Rn concentration is only about 2 kBq/m^3. This electronic detector ensemble is of particular importance for those remote volcanic and desert areas where radon evaluation in situ means an additional effort for collecting the data; but as it shown careful analysis have to be made for right interpretation of data.

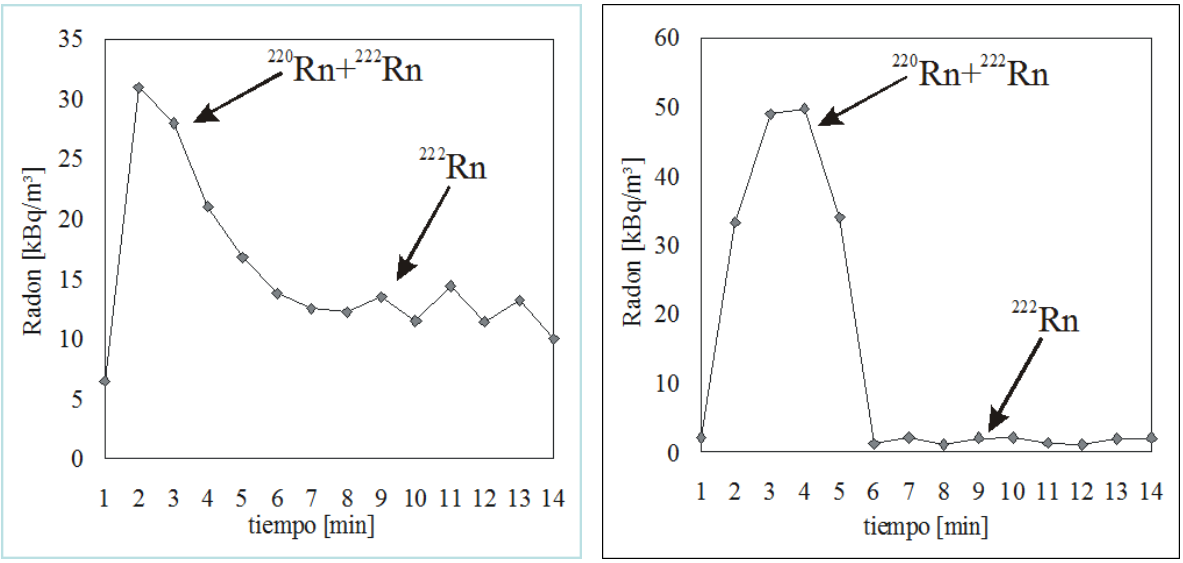

Figure 7.- Removal of ^{220}Rn contribution for ^{222}Rn evaluation by ^{220}Rn decay effect in the AlphaGUARD detector.

3.2 Grid of radon sampling

Typical exploration areas in geothermal fields cover several km^2 making necessary the optimization of the sampling grid, no to over sampling the field nor to lose data. A geo statistical approach is a useful tool to test the right size of sampling grid [Balcazar 1997]. The method consist in a radon sampling with a particular grid size, then a correlation of each point to all the rest is plotted in a semivariogram. A fitted curve shows on the inflection point up to what extent the correlation between points is lost. The semivariograms can be selectively chosen in a desire direction.

Los Azufres geothermal field with an installed geothermal energy capacity of 200 MW, is use here to exemplify the grid size studies for radon distribution. The field covers a total area of about (18 x 13) km^2; it is mainly dividing into three zones: two production zones at the South and North; and an exploration zone at the North-West. Figure 8 shows the rectangular grid of 141 points (black dots) in an array of (500 x 500) m^2, in the South part of the Los Azufres field, covering a smaller area of (8 x 5) km^2. This array was initially chosen in mutual according with the needs of CFE. Each sampling point is geo positioned using a Geo Positioned System (GPS) and the resulting radon concentration (kBq/m^3) for each point is shown on each sampling point.

In Figure 8 the GIS software do not draw lines on points of equal radon concentration values but rather draw distribution probability areas of radon concentration in the survey zone. The blue numbers inside the areas in Figure 8 means what percentage of all radon values in that area have concentrations above the median of field (34.73 kBq/m^3 for this case); the darker the color the higher the radon concentration probability. It is useful to plot the probability radon distribution in this mode because from those percentages a fast idea and criteria of radon anomalies in the geothermal field can be established.

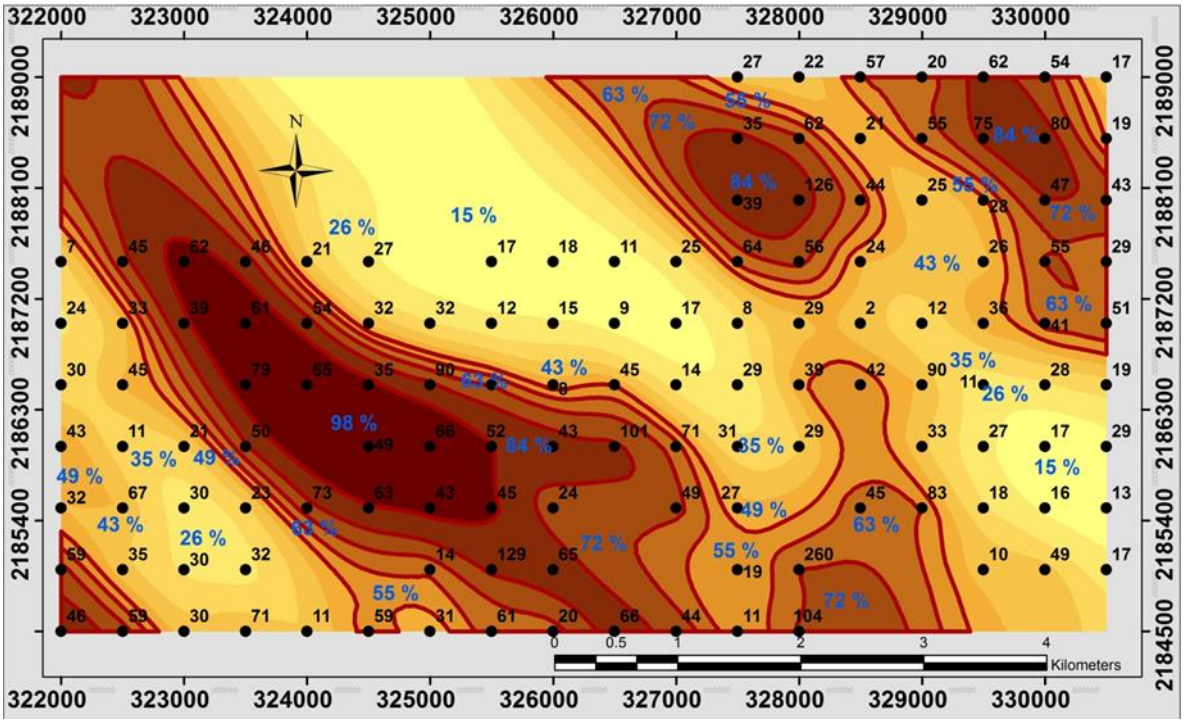

Figure 8.- South zone, Los Azufres Geothermal field. Radon concentration is in black numbers; areas defining the percentage of radon values above the median (34.73 kBq/m^3) in that area.

A frequency distribution of radon for the survey zone is shown in Figure 9 (left), and the associated typical log-normal frequency distribution at right in Figure 8. 50% of the radon concentration values are higher than the media of 34.73 kBq/m^3.

A geostatistical analysis to data as part of the GIS software, produce a set of semivariograms showing maximum radon gradient in the direction South-West to North-East and the minimum radon variation in the North-West South-East, with a maximum of correlation distance about 1000 m and around 2000 m respectively, which means that the field was initially over sampled. Data of twelve detectors were lost in the sampling grid; however because the size of this correlation distances the loss of this data does not affect significantly the radon pattern.

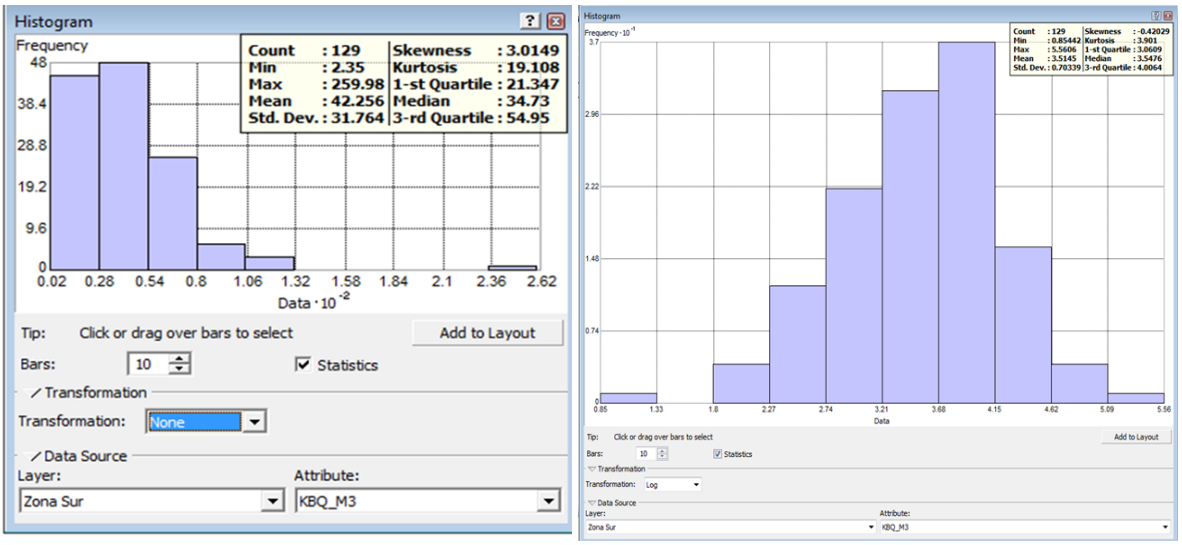

Figure 9.- South Zone of Los Azufres, 50% of radon values are higher than 34.73 kBq/m^3. Left: frequency distribution of radon concentration, Right: Associated typical log-normal frequency distribution.

4.- RESULTS AND DISCUSSION

Part of the results obtained from the studies performed in three geothermal fields, Los Azufres, Tres Vírgenes and Los Humeros are used here for giving answer to some relevant questions of the applicability of radon as geothermal indicator, the reproducibility in the field, its association to faults, and its association to resistivity characteristics of the field.

4.1 Radon, indicator of geothermal activity

The three study zones of Los Azufres are displayed in Figure 10 (red rectangles) and the total of the 313 points (black dots) are included in a GIS analysis. The distribution probability areas of radon concentration shows enormous differences for the three zones; at least 90% of the area in the south part have values greater than the median for of whole field (6.88 kBq/m^3); in the north zone most of the radon points are in an area having at least a 72% of radon concentration values greater than the median; a big contrast is observed in

non-producing zone at the North-West, where all radon values in the whole zone are less than 2% of the media.

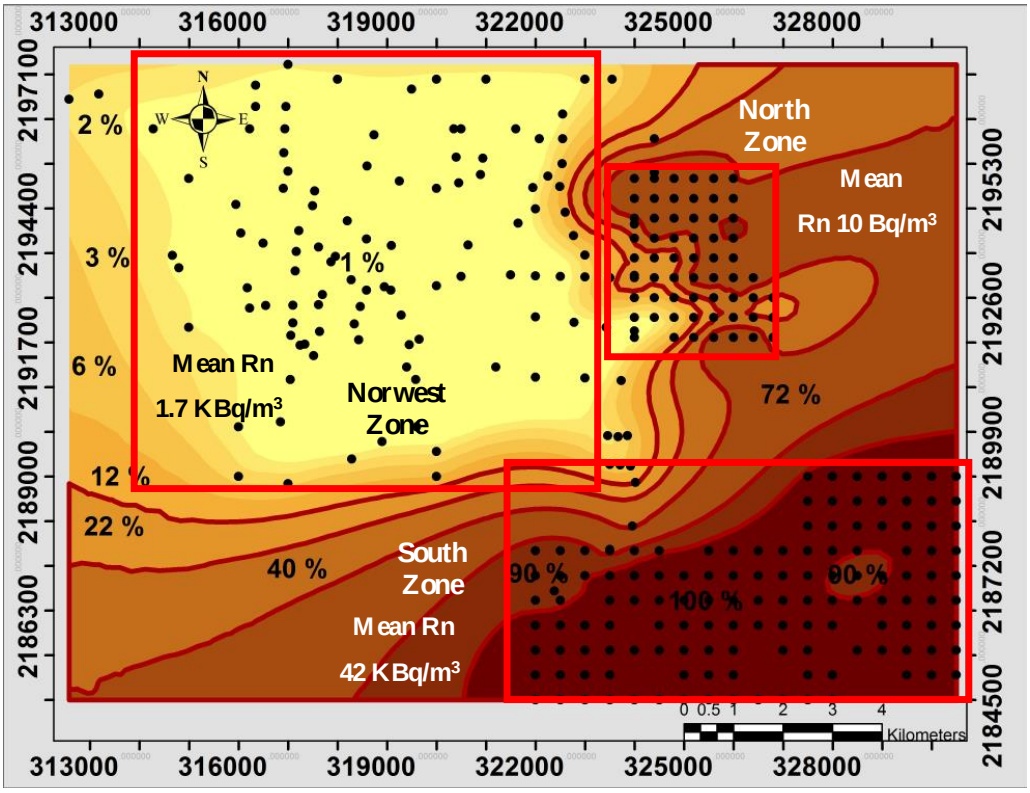

Figure 10.- Radon probability distribution for the three study zones of Los Azufres geothermal field: North, South and North-West. The median is 6.88 kBq/m^3.

There is a clearly indication of permeability and or geothermal activity for the two producing zones, being bigger at the south than at the north. There is no a clear geothermal connection between both producing zones (south and north) therefore, it is not right to include all the points in a single analysis as the one displayed in Figure 10 and even it is wrong to include the non-producing zone (North-West) because those experimental results do not have the same underground origin. The resulting frequency radon concentration distribution for the whole field is shown in Figure 11 (left) and the associated log-normal frequency distribution (Figure 11, right) show the absence of the expected normal distribution. The right way of data treatment in this case is to consider each zone individually as it was made in section 4.1 for the south zone obtaining a mean radon

concentration of 42 Bq/m^3, 10 Bq/m^3 for the north zone alone and 1.7 Bq/m^3 for the North-West zone.

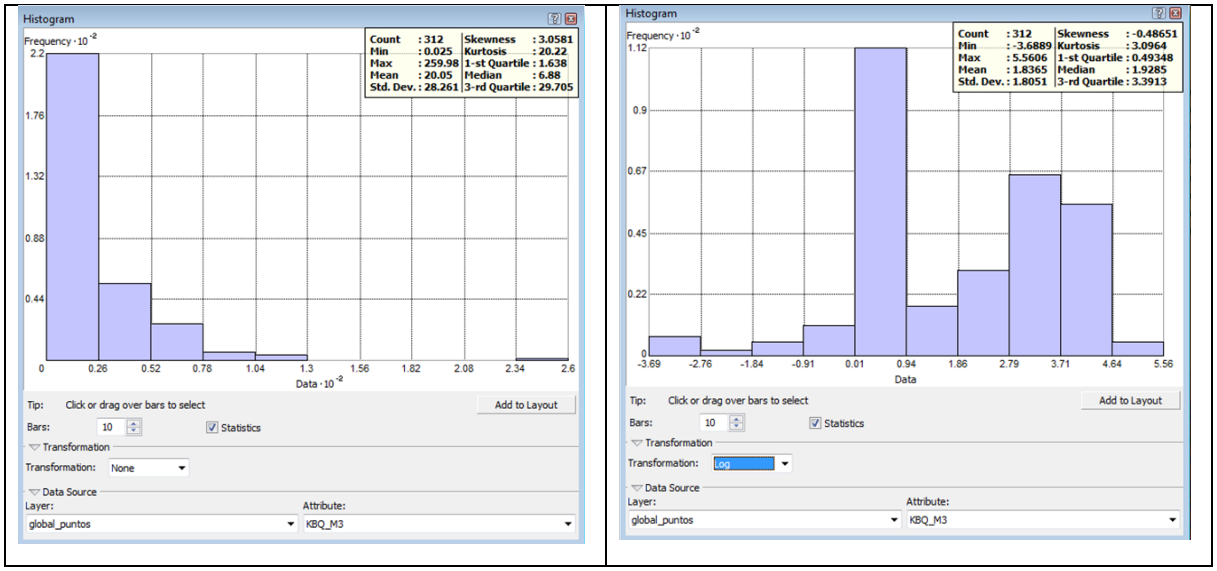

Figure 11.- Three zones of Los Azufres , 50% of the radon values are bigger than 6.88 kBq/m^3. Left: frequency distribution of radon concentration. Right: Associated log-normal frequency distribution.

4.2 Radon reproducibility

To test the reproducibility of radon signal in an active geothermal field, the north zone of (3.2 x 2.8) km^2 at Los Azufres geothermal field was selected. The selected rectangular grid size had 400 m x 400 m. Four individual sampling campaigns were performed one month apart, this time is long enough to reduce radon concentration interference down to less than 1% from the previous campaign (7.8 half-lifes) and it is sufficiently short not to produce mayor changes in the geothermal activity of the hot reservoir underground the sampling zone.

The survey was performed during the dry season from November to February to avoid undesired heavy-rain interference usually present at the middle of the year. The results of three measuring campaigns are displayed in Figure 12.

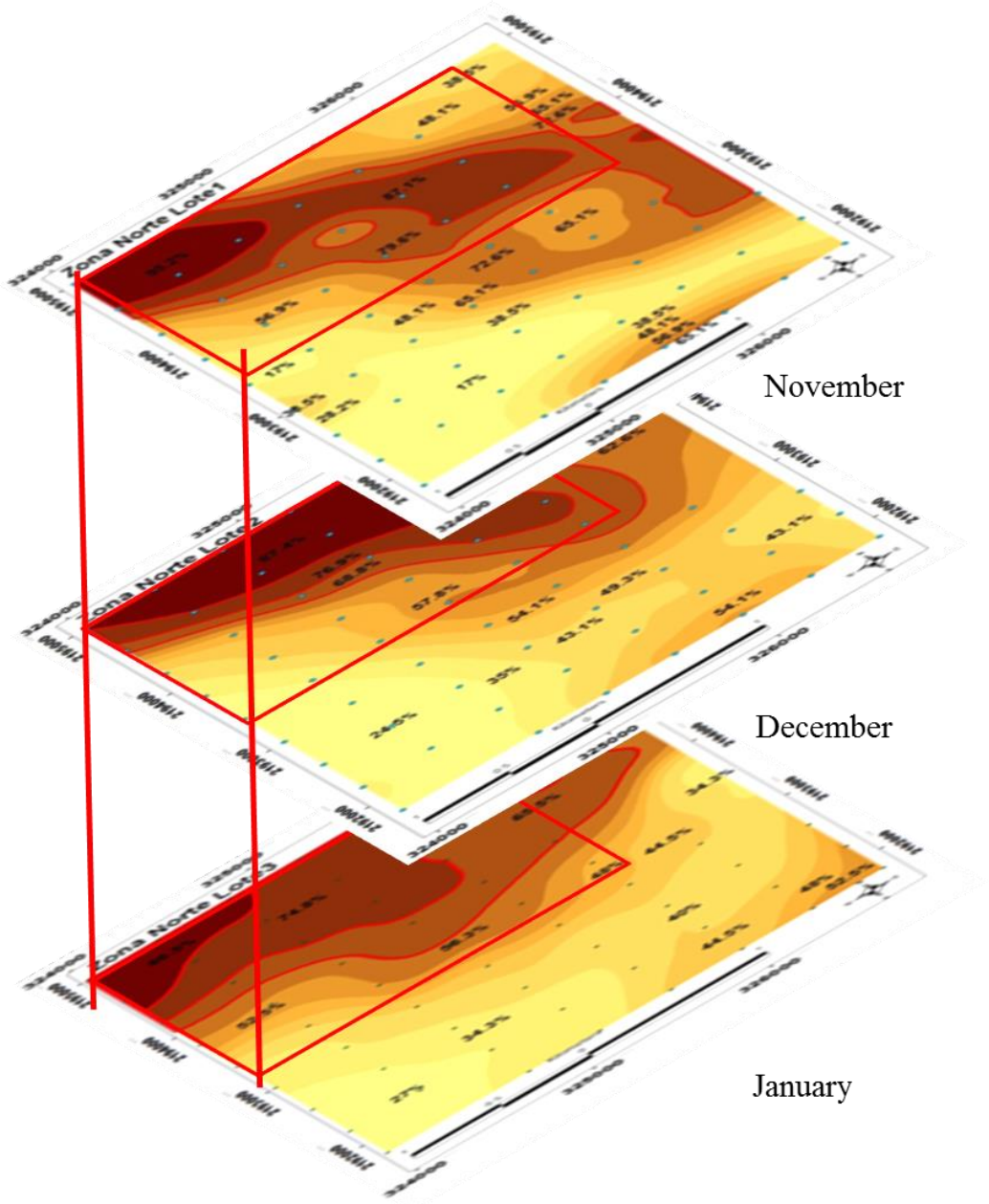

Figure 12.- Three monthly radon sampling campaigns, north zone of Los Azufres. Systematically bigger permeation at North-West than South-East side.

The median radon concentration values for the sampling in November, December and January were all similar, 6.4, 6.8 and 11.9 kBq/m^3 respectively. Either the radon permeability or geothermal activity was systematically present with higher probability at the North-West in all samplings campaigns, as indicated with red rectangles in Figure 12. Minor radon concentration probability was also systematically showed at the South-East.

Considering the complex of physical, geophysical, and geochemical variables involved in a geothermal reservoir due to the thermo dynamical properties, water-rock interaction affecting the geochemical properties and therefore de gas carriers of radon to the earth surface, one not should expect to have a correspondence one to one for each sampling period as it happens in repetitive controlled experiments in laboratory.

4.3 Radon related to faults

The geothermal field of Tres Virgenes with an installed capacity of 10 MW, is located southeast of the three volcanic edifices known as Three Virgins, which provide the geothermal activity of the site. The producing zone of the field is located at the southeast of volcanoes in a site of faults system orientated in the North-South direction. Figure 13 indicates the name and the orientation of the fault system (black lines) that span both sides of the volcanoes.

A study of field permeability was undertaken in a new area to the North-East of the volcanoes. Together with CFE two grids for radon sampling were defined, one in the producing zone and another in the new zone of exploration (black dots in both areas). The objective of this study was to determine the permeability in a new zone to the North-West of the volcanic structures that would allow exploration drilling for finding a new energy production area. Detailed results will be reported in another paper.

The median of radon concentration for the whole values was 3.8 kBq/m^3; the areas containing the probability distribution of radon concentration are displayed in Figure 13 where the darker the areas the higher the probability of radon concentration. The areas of major probability and their alignment are with the known faults system El Partido (71%), El Partido 2 (62%) and El Viejo (62%), that were previously determined in the geothermal field. Results indicate the lack of continuousness of faults El Volcán 1 and El Volcán 2 towards the North-West direction; the conceptual model explained in Figure 3 fully apply in this case as indicated by the low permeability values.

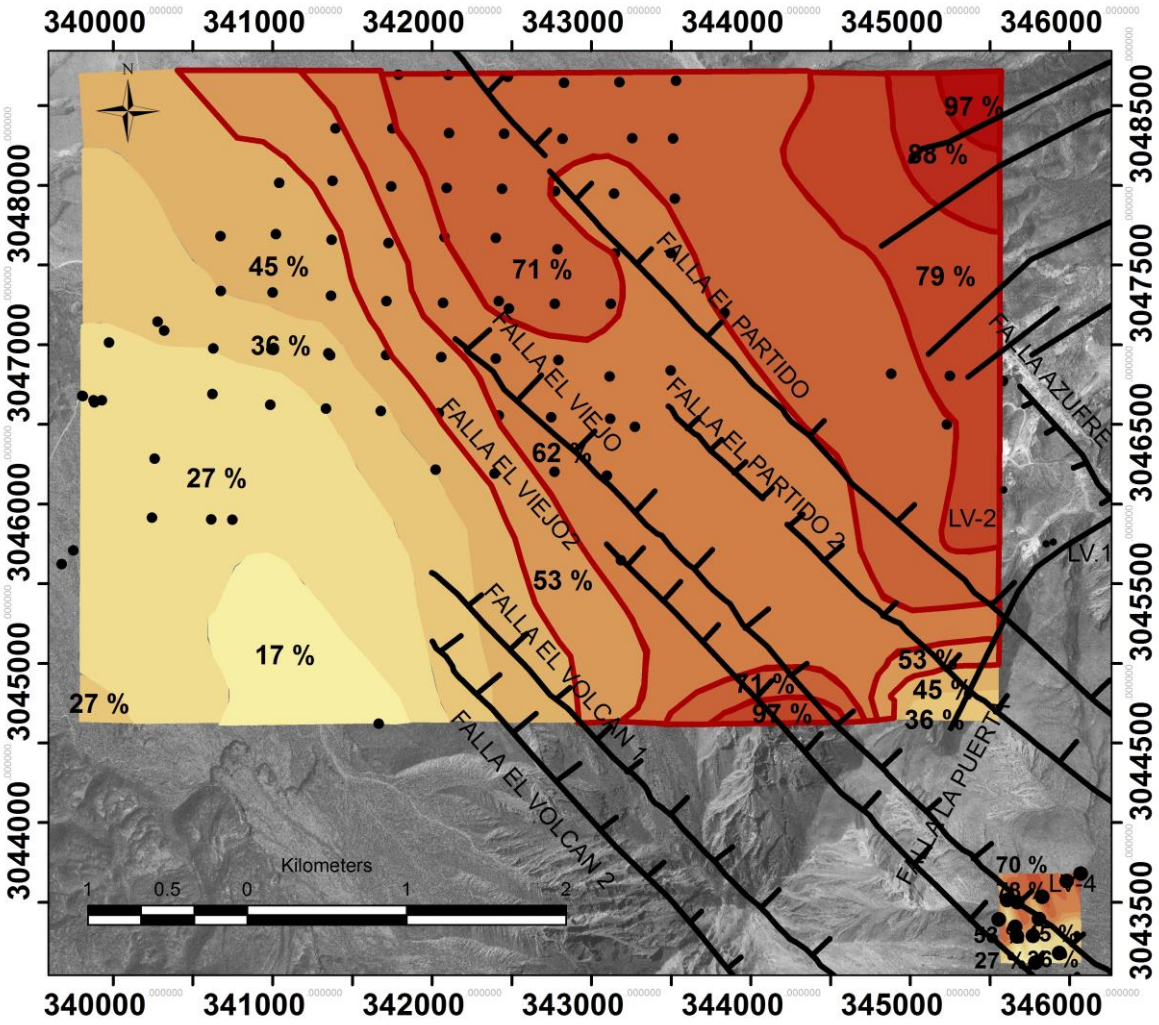

Figure 13.- Tres Virgenes geothermal field: producing zone small area at South-East; new exploration zone big area at North-West.

4.3 Radon related to resistivity

Los Humeros geothermal field belong to a caldera composed by two collapsed regions: Los Potreros and Xalapasco. The field has an installed energy capacity of 40 MW from producing wells that are aligned in the North-South direction close to Los Humeros fault, as indicated in Figure 14. The caldera has high presence of lava from volcanic eruptions and absence of hydrothermal springs, which preclude the prospecting by geochemical analysis of groundwater. The use of radon for determining permeability in this field was a challenge.

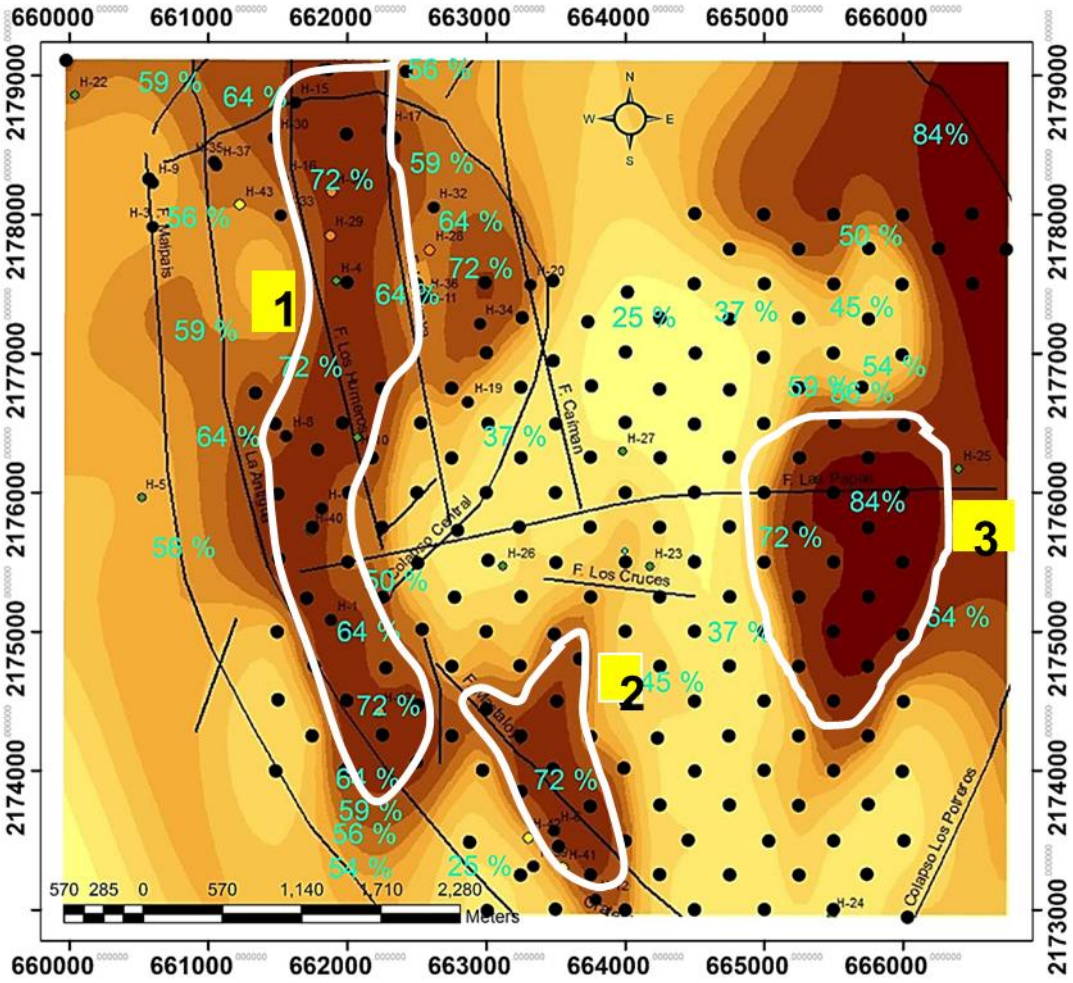

Figure 14.- Probability radon distribution at Los Humeros geothermal field.

The grid for radon determination as convened with CFE consisted of 200 points from which radon concentration was measured. The median value for all measurements was indeed low of just 1.08 Bq/m^3; however, the relative probability radon distribution shows the highest values in three areas, delimitated by the white lines in Figure 14. Area number 1 corresponds totally to all producing geothermal wells with 72% of the radon probability concentration and it is in right alignment to the set of faults belonging the boundary Xalapasxco collapse. New areas 2 and 3 are identified to have 72% and 84% radon probability distribution respectively with promising prospecting plans for geothermal exploration. Detailed discussion will be given in a paper under preparation.

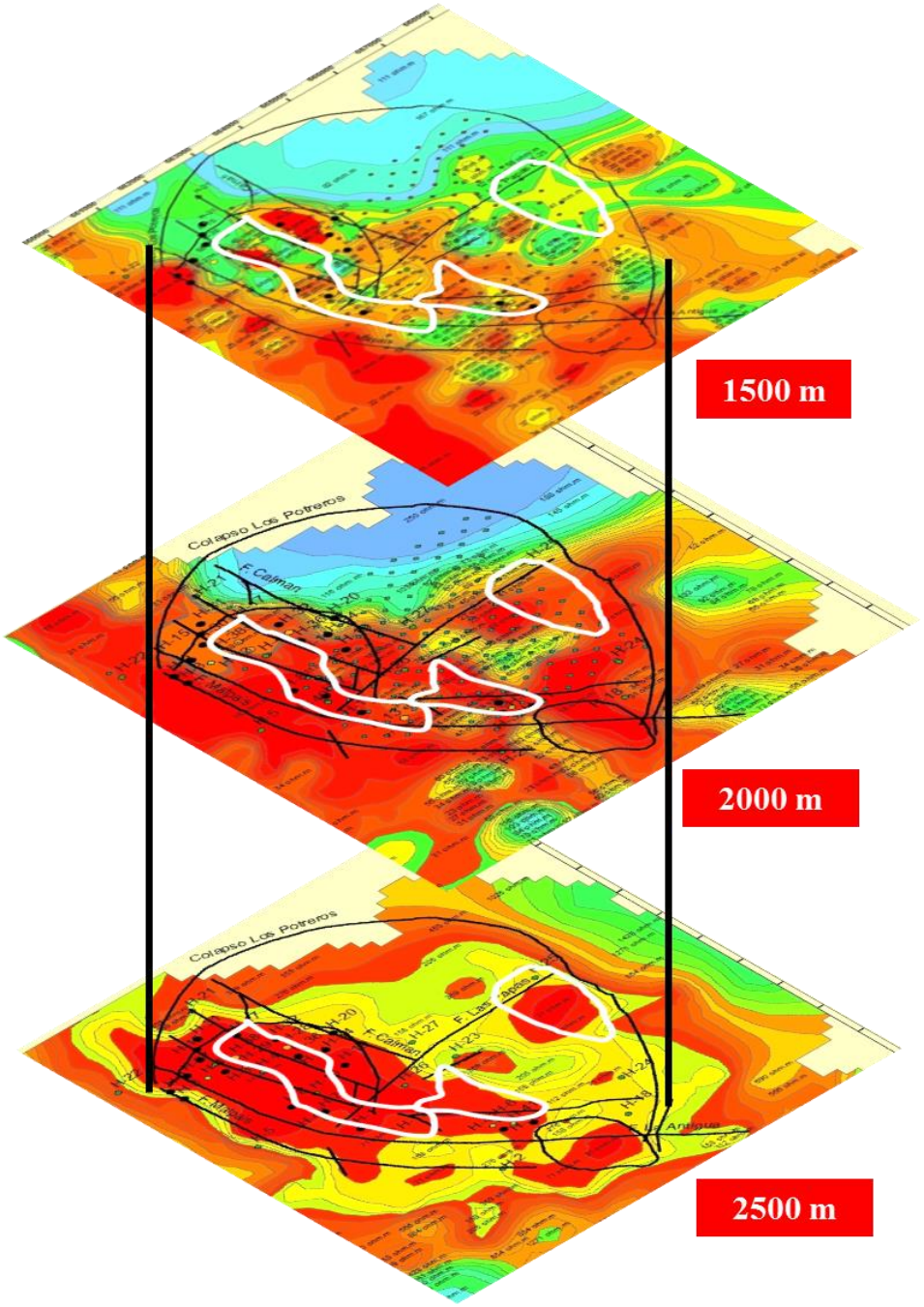

Figure 15.- Surface radon intersection areas (white lines) and conductivity (red colors) at three depths at Los Humeros geothermal field.

Resistivity studies were previously performed at Los Humeros by CFE at several depths 2550 m 2000 m and 1500 m, results are displayed in Figure 15; the intensity of red color for the three depths means the degree of conductivity (inverse of resistivity). The shape of

three areas (white color) of high radon concentration probability determined in Figure 14, overlap the conductivity maps. Although radon is determined at the surface there is a high correspondence of radon with conductivity property previously obtained at 2500 m; even the correspondence holds at 2000 m. The presence of volcanic material mentioned above reduce the ascendance of salinity compounds from the geothermal reservoir up to the surface, in such a degree that if conductivity analysis were performed at maximum depths of 1500 m, wrong conclusion could be derived. The conceptual model explained in Figure 2 fully apply in this case, because although the field has low permeability, the relative permeable values clearly show the geothermal activity of the reservoir.

5.- CONCLUSIONS

Agreements of radon probability distribution to geothermal activity (Los Azufres, Figure 10), open faults (Tres Virgenes, Figure 13; Los Humeros, Figure 14) and resistivity (Los Humeros, Figure 15) have experimentally obtained in three geothermal fields.

None of the exiting geophysical, geochemistry or geological exploration methods can alone describe a possible geothermal activity; then high permeability areas determined by radon anomalies in field gives the best results when they are correlated to all exiting data from several earth sciences disciplines (magnetometry, gravimetry, telluric, electrical resistivity, and geology) and this correlation should be interpreted together with the users (CFE in this paper). The relationship of these parameters, provide a powerful diagnosis of the presence of the geothermal potential of the field, which identifies the area of greater permeation for drilling.

Radon anomalies in the field indicate the recent thermodynamic underground due to the ^{222}Rn short highlife (3.82 days) and considering the complex lithology, faults and fractures present underground the geothermal field a good reproducibility of radon anomalies is obtained in the same geothermal area at different times (Los Azufres, Figure 12).

In summary, measurements of resistivity, seismic monitoring, and gravimetry previously made confirm the geothermal activity in those areas of high permeability as determined by the Radon distribution probability.

Acknowledgments

To Gerencia de Proyectos Geotermoelectricos, CFE, for focusing the goals of present results, technical support for fieldwork and fruitful discussions during and after performing the experimental work. To the technical support by Oliver Gutiérrez, Miguel Mejía, Francisco Cruz, Sergio Arredondo, Octavio Vázquez, Antonio Anastasio, Arturo Serrano, Delia Chávez and Juan Carlos Torres.

REFERENCES

Akerblom G; Mellander H. *RADON MEASUREMENTS BY ETCHED TRACK DETECTORS*. World Scientific. (First edition, 1997).

Balcazar M; Chávez A (1984). *A modified version of a spark counter for α-spectrosocpy.* Nuclear Tracks and Radiation Measurements **8**: 617-620.

Balcazar M; Santoyo E; González E; González D. (1991). *Radon measurements in heat-producing geothermal wells.* Nuclear Tracks and Radiation Measurements **19**: 283-287.

Balcazar M; González E; Ortega M; Flores JH; Faz P; Renteria D; Torres V (1993). *Geothermal energy prospecting in El Salvador.* Nuclear Tracks and Radiation Measurements **22**: 273-276.

Balcazar M. *RADON MEASUREMENTS BY ETCHED TRACK DETECTORS*. World Scientific, (First edition, 1997).

Balcazar M. [online]. *Radiación inducida y natural, Actividad Científica y Tecnológica en el Instituto Nacional de Investigaciones Nucleares*. (2008). Homepage of the National Institute for Nuclear Research< http://www.inin.mx/ >. [Reviewed on December 2013].

Jönsson G. *RADON MEASUREMENTS BY ETCHED TRACK DETECTORS*, World Scientific, (First edition, 1997).

Schubert M; Peña P; Balcazar M; Meissner R; López A. (2005). *Determination of radon distribution patterns in the upper soil as tool for the localization of sub-surface NAPL contamination.* Radiation Measurements **40**: 633-637.

Maya-González R. (2007). *La geotermia y fuentes alternas en la generación de energía eléctrica*. Tercer Congreso Nacional de la Academia de Ingeniería. México DF.

Santoyo E; Barragán RM. (2010). *Energía geotérmica Revista*. Academia Mexicana de Ciencias **61:** 40-51.

Van de Graff ER; Van der Spoel WH; de Meijer RJ. *RADON AND THORON IN THE HUMAN ENVIRONMENT*. World Scientific, (First edition, 1997).